The domain is whatever I want it to be

Conformal mapping methods and potential flow problems

Math 704 Final Project

Carsen Grote*

May 7, 2024

1 Introduction

1.1 Potential Flow

Problems in fluid dynamics commonly arise from wanting to find the steady velocity field for a two dimensional, irrotational, inviscid, and incompressible fluid. Writing the velocity field of the fluid as $\mathbf{u} = (u, v)$, the incompressible and irrotational properties of the fluid are enforced by the constraints

$$\frac{\partial u}{\partial x} + \frac{\partial v}{\partial y} = 0, \tag{1}$$

$$\frac{\partial v}{\partial x} - \frac{\partial u}{\partial y} = 0. \tag{2}$$

The incompressibility can be immediately satisfied by writing the velocity as

$$\mathbf{u} = \nabla^{\perp}\psi = (\frac{\partial \psi}{\partial y}, -\frac{\partial \psi}{\partial x}) \tag{3}$$

for some unknown, continuously differentiable function ψ. In a similar way the irrotational requirement can be satisfied by writing the velocity as

$$\mathbf{u} = \nabla\phi = (\frac{\partial \phi}{\partial x}, \frac{\partial \phi}{\partial y}). \tag{4}$$

for another unknown, continuously differential function ϕ. Here ψ and ϕ are known as the velocity potential and stream function, respectively [1]. It can also be easily shown from equations 1-4 that ψ and ϕ satisfy Laplace's equation. More interestingly, from the relationship of the

*Department of Mathematics, University of Wisconsin-Madison

partial derivatives of ϕ and ψ, we see that

$$u = \frac{\partial \psi}{\partial y} = \frac{\partial \phi}{\partial x}, v = -\frac{\partial \psi}{\partial x} = \frac{\partial \phi}{\partial y}, \tag{5}$$

thus ψ and ϕ satisfy the Cauchy-Riemann conditions and define an analytic complex function $\Omega(z) = \phi(x, y) + i\psi(x, y)$, known as the complex velocity potential [2]. With $\Omega(z)$ the velocity field can be retrieved by taking the conjugate of the derivative,

$$\overline{\Omega'(z)} = \frac{\partial \phi}{\partial x} + i\frac{\partial \phi}{\partial y} = u + iv. \tag{6}$$

Unlike standard flows where viscosity induces a no-slip boundary condition, for inviscid potential flows the boundary condition is that the normal component of the fluid velocity must vanish on a rigid boundary:

$$\nabla \phi|_{\partial\Omega} \cdot \hat{n} = \mathbf{0}, \tag{7}$$

where $\hat{n}$ is the outward normal vector from the rigid boundary (no penetration). Additionally, since $(\phi_x, \phi_y) = (\psi_y, -\psi_x)$, or $\nabla\phi \cdot \nabla\psi = 0$ at every point, we see that the direction of the fluid flow is perpendicular to the gradient of the stream function. Thus the level curves of the stream function align with the direction of the flow field everywhere and are called streamlines of the flow [2]. Therefore we have reduced the problem of finding the velocity field of the fluid to finding any differentiable, complex function $\Omega(z)$ on our domain that satisfies the boundary conditions. Further, since ϕ and ψ are harmonic conjugates the problem is further reduced to finding a harmonic function $\phi(x, y)$ on our domain that satisfies a Nuemann condition on the boundary.

1.2 Conformal Mappings

When solving two dimensional potential flow problems described above, the geometry of the domain normally incurs all of the difficulty in finding the harmonic function ϕ that satisfies the boundary conditions. For non-standard domains it then becomes natural to ask the question "Why don't I just find the solution on a simpler domain and *map it* to my complicated domain?". This is the driving idea behind the use of conformal mappings in potential flows and other problems.

The key quality of conformal mappings is that they are angle preserving transformations [2]. Here we follow the arguments given in Ablowitz and Fokas (p. 312-320) to analyze the qualities of conformal transformations [2]. Consider the mapping $w = f(z)$ from the z plane to the w plane with f an analytic function of z. If $z(s)$ curve in the z plane parameterized by arc length s, then under $f(z)$ it is mapped to the curve $w(s)$ in the w plane. The tangent line to $w(s)$, w_s,

at the point $s_0 = f(z_0)$ is then given as

$$w_s(s_0) = f'(z_0)z_s. \tag{8}$$

Writing this as a complex eponential and considering the argument gives:

$$\arg(w_s) = \arg(f'(z_0)) + \arg(z_s). \tag{9}$$

Thus the curve $z(s)$ passing through z_0 is rotated by an angle of $\arg(f'(z_0))$ under the mapping $f(z)$, so long as $f'(z) \neq 0$ [2]. Moreover, any two curves passing through a point z_0 in the z plan are both rotated counterclockwise by the same magnitude under the mapping $f(z)$ and thus intersect at the same angle in the w plane [2]. While angles are preserved under conformal mappings, it is important to note that lengths are not [2]. This can be seen by considering the modulus of (8),

$$|w_s(s_0)| = |f'(z_0)||z_s|, \tag{10}$$

which shows that curve lengths are scaled by a factor of $|f'(z)|$ [2]. If $f'(z) = 0$, then the transformation $f(z)$ ceases to be conformal and such point is called a critical point of f [2]. To understand what happens at a critical point z_0 geometrically, consider a small line segment $z_0 + \delta z$. The corresponding line segment under the mapping, $\delta w = f(z_0 + \delta z) - f(z_0)$, can be analyzed by Taylor expanding $f(z_0 + \delta z)$ about $f(z)$,

$$\delta w = f(z_0 + \delta z) - f(z_0) = (\delta z)f'(z_0) + \frac{1}{2}(\delta z)^2 f''(z_0) + ... \tag{11}$$

If $f^{(n)}(z_0)$ is the first non-vanishing derivative at z_0, then we have that

$$\arg(\delta w) \approx n\arg(\delta z) + \arg(f^{(n)}(z_0)). \tag{12}$$

This shows (without proof) that the angle between any two intersecting line segments at a critical point z_0 is scaled by a factor of n under the mapping $f(z)$ [2]. Before moving into example problems and methods, we wish to note two critical theorems on conformal mappings.

Theorem 1 *Let C be a simple closed contour enclosing a domain D, and let $f(z)$be analytic on C and in D. Suppose $f(z)$ takes no value more than once on C. Then (a) the map $w = f(z)$ takes C enclosing D to a simple closed contour C^* enclosing a region D^* in the w plane; (b) $w = f(z)$ is a one-to-one map from D to D^*; and (c) if z traverses C in the positive direction, then $w = f(z)$ traverses C^* in the positive direction.*

The proof of this theorem is given in Ablowitz and Fokas (p. 343) [2]. The first result of the theorem tells us that conformal maps preserve the connectivity of a domain, and map open sets in the z domain to open sets in the w domain [2].

Theorem 2 ***(Riemann Mapping Theorem)*** *Let D be a simply connected domain in the z plane, which is neither the z plane or the extended z plane. Then there exists an analytic and one-to-one function $f(z)$, such that $w = f(z)$ maps D onto the disk $|w| < 1$.*

This theorem is non-constructive, but strikes the point that we will emphasize later on that most conformal mapping problems revolve around mapping a complicated, simply connected domain to the unit disc or upper half plane. The proof of this theorem can be found in the textbook by Nehari [3]. The Riemann Mapping Theorem only applies to simply connected open sets, but the Osgood-Carathéodory Theorem shows that the mapping f to the open unit disc can be extended such that it is continuous and injective on the boundaries [4]. It has also been shown, via bilinear transformations, that the unit circle can be conformally mapped onto the upper half plane [2]. Therefore we could also state the the result of the Riemann Mapping and Osgood-Carathéodory theorems with respect to the upper half plane. Lastly, the correspondence of only three points on the boundaries of the two domains can be chosen arbitrarily [2]. Once three points on each boundary have been selected, i.e. choosing $w_i = f(z_i)$ for $i = 1, 2, 3$, the resulting map $f(z)$ becomes unique. Although we could consider many more important theorems of conformal mappings, let us continue to putting what we already know to work.

2 Motivating Examples

We start with two examples of using conformal mappings to find the potential flow on non-standard domains. The first example considers the flow due to point sources and sinks within a rectangular container of infinite height while the second example examines flow past a slit.

Consider a rectangular container of infinite vertical height in the z plane with its base centered on the real axis with a length of π. The two corners of rectangle not at infinity then lie at $z = \pm\pi/2$. Our goal is to find the fluid velocity near the bottom of the container with a point source and point sink on the bottom boundary[1]. As stated above, we start by finding a conformal map from our infinite rectangle domain to a simpler domain in the w plane. Here we choose the upper half-plane. Consider the mapping

$$w = f(z) = \sin(z). \tag{13}$$

$f(z)$ opens the sides of the rectangle to the upper half plane. This is analytically seen at the two corners of the rectangle where $f'(\pm\pi/2) = \cos(\pm\pi/2) = 0, |f''(\pm pi) = 1|$. Referring to equation (12), since the second derivative of f is non-zero at the corners, angles are indeed increased by a factor of two which opens the corner to a straight line on the half plane. The corners themselves

[1]The author and his advisor, Saverio Spagnolie, came up with this example while passing time during a car ride together. We were interested in modeling the flow of a supersaturated fluid like carbonated water in a rectangular container where the point sources and sinks mimic the effect that the growth of CO_2 bubbles on the bottom of the container have as they force fluid flow.

are mapped to $w = \pm 1$, respectively, and any point on the real axis in the z plane between them is mapped to the real axis between -1 and 1 in the w plane. The infinite sides of the container are also mapped to the real axis,

$$\sin(\pm\pi/2 + iy) = \pm\cos(iy) = \pm\frac{e^{i(iy)} + e^{-i(iy)}}{2} = \pm\frac{e^{-y} + e^{y}}{2}. \tag{14}$$

Our only boundary condition in the w plane is that the flow is perpendicular to the boundary on the real axis, or equivalently that ψ is constant on the real axis. Additionally, lets add a point source at $z = c$ and point sink (for mass conservation) at $z = -c$ in the z plane with strength 2π on the real axis to give a unique solution with non-zero flow. For the point source with strength 2π placed at $z = c$, the velocity away from the point in the w plane must be $1/(w - f(c))$ in the radial direction [5]. This leads to finding the fluid velocity in the w plane due to the single point source as

$$\overline{\Omega'(w)} = u + iv = \frac{1}{w - f(c)}. \tag{15}$$

Integrating once gives the complex potential

$$\Omega(w) = \log(w - f(c)) = \phi(x, y) + i\psi(x, y). \tag{16}$$

Since $\Omega(w)$ is constantly real on the real axis, it must be that $\psi(x, y = 0)$ is constant zero on the real axis which makes it a streamline as desired. We can add the point sink at $z = -c$ with strength 2π in a similar manner, with flow going into the point as $-1/(w + f(c))$ in the radial direction. This leads us to the final velocity and potential for the flow on the w plane as

$$\overline{\Omega'(w)} = u + iv = \frac{1}{w - f(c)} - \frac{1}{w + f(c)}, \tag{17}$$

$$\Omega(w) = \log\left(\frac{w - f(c)}{w + f(C)}\right) = \phi(x, y) + i\psi(x, y). \tag{18}$$

The last part is to use our conformal map $w = \sin(z)$ to map our infinite rectangular container in the z domain to to the half plane w domain and evaluate the solution there,

$$\Omega(z) = \log\left(\frac{\sin(z) - \sin(c)}{\sin(z) + \sin(c)}\right). \tag{19}$$

See Fig. 1 for the visualized fluid flow. For a contrasting example we will analyze uniform potential flow past a thin wing. We start with the classical 'Circle Theorem' by Milne-Thompson which states that if $w = f(z)$ is a complex potential with no singularities in $|z| \leq a$, then $w = f(z) + \overline{f(a^2/\bar{z})}$ is a complex potential of a flow with the same singularities as $f(z)$ in $|z| > a$ and $|z| = a$ as a streamline [5]. The second part of the theorem can be seen after writing $z = ae^{i\theta}$,

$$w = f(ae^{i\theta}) + \overline{f(a^2/ae^{-i\theta})} = f(ae^{i\theta}) + \overline{f(ae^{i\theta})}. \tag{20}$$

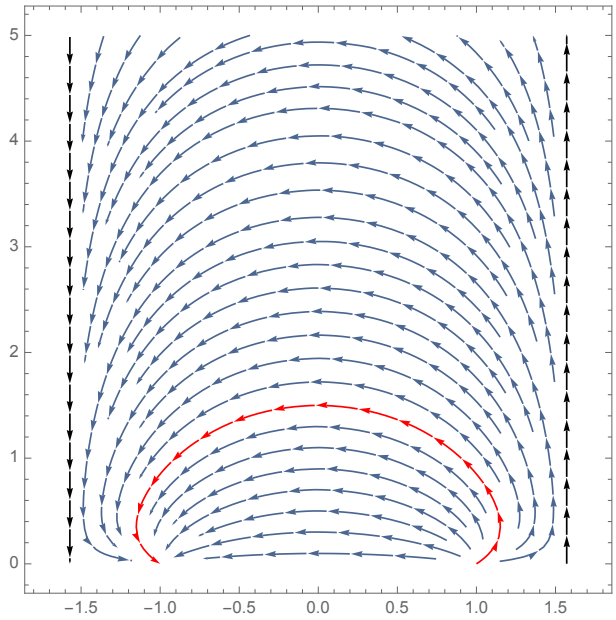

Figure 1: Potential flow in a infinitely tall rectangle with base length of π centered on the real axis with a point source and sink at $z = \pm 1$, respectively with strengths of 2π. The container boundaries at $x = \pm\pi/2$ are shown by the black streamlines.

Therefore w is real on $|z| = a$, so $\psi = 0$ thus $|z| = a$ is a streamline [5]. This provides a simple way to solve for the flow around a circle of radius a given a background potential flow $f(z)$. From here we proceed to finding the flow about a slit as in Acheson (p. 137-138) [1]. Let the slit in the z plane have length $4a$, lying on the real axis with ends at $z = \pm 2a$, respectively. The crux of the problem is to find a conformal map that maps the slit in the z plane to a circle with radius a in the w plane, for which we know how to find flow around. This conformal map is (not so intuitively) given by

$$w = f(z) = \frac{1}{2}(z + \sqrt{z^2 - 4a^2}), \tag{21}$$

and is conformal everywhere in the fluid. Satisfying that the slit in the z plane is a streamline in the resulting flow requires that the flow found in the w plane has $|w| = a$ as a streamline. Back to the circle with radius a in the w plane, a constant background flow of speed U at an angle α with the positive real axis is obtained with the potential $\widetilde{\Omega(w)} = Ue^{-i\alpha}w$. With the circle theorem we then have that

$$\Omega(w) = Ue^{-i\alpha}w + \overline{\left(\frac{Ua^2e^{-i\alpha}}{\overline{w}}\right)} = Ue^{-i\alpha}w + \frac{Ua^2e^{i\alpha}}{w}. \tag{22}$$

is a potential for uniform flow $Ue^{i\alpha}$ past a circle of radius a with $|w| = a$ as a streamline. Combining our conformal map from the slit to the circle (21) with our potential flow around the circle (22) delivers us the potential for the same uniform flow past the slit in z plane with

the slit as a streamline,

$$\Omega(z) = U\left[\frac{1}{2}e^{-i\alpha}(z+\sqrt{z^2-4a^2}) + \frac{2a^2e^{i\alpha}}{z+\sqrt{z^2-4a^2}}\right]. \tag{23}$$

Since $\Omega(w)$ is analytic and $f(z)$ is conformal, we have that $\Omega(f(z))$ is also analytic [2]. Analyzing the derivative of Ω will give us insight into the flow velocity about the slit,

$$\Omega'(z) = \Omega'(f(z))f'(z), \tag{24}$$

$$f'(z) = \frac{1}{2} + \frac{z}{2\sqrt{z^2-4a^2}}. \tag{25}$$

As $f'(z)$ becomes infinite at $z = \pm 2a$, the velocity of the fluid is then infinite at the two ends of the slit. Though beyond the scope of this report, we can smooth out the flow at one of the ends of the slit by adding a circulation flow of the form $\Gamma/(2i\pi w)$ with an appropriate Γ. This is known as the Kutta Condition, and maintains the circle as a streamline [6].

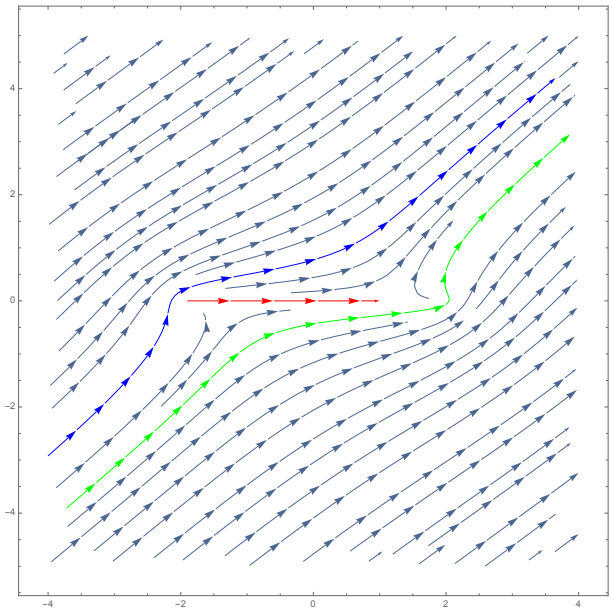

Figure 2: Uniform potential flow past a slit (red) of length 4 and centered on the real axis.

3 The Hodograph Method for Free Streamlines

The lack of viscosity in potential flow allows for the formation of streamlines that separate fluid in motion from fluid at rest, called free streamlines [5]. The introduced difficulty here is that the exact locations of free streamlines in a flow are not immediately apparent and require some analysis to find. These streamlines are given by the level curves of the stream function ψ in the

complex potential. We can appeal to Bernoulli's theorem for steady potential flows which states that

$$H = \frac{P}{\rho} + \frac{1}{2}|\mathbf{u}|^2 \tag{26}$$

is constant along streamlines in flows without external forces [5]. Here P, ρ, and $\mathbf{u}$ are the fluid pressure, density, and velocity respectively. The pressure field in the flow must be continuous so the pressure on a free streamline must be equal to the pressure on the adjacent, stagnant fluid which has constant pressure [5]. Therefore the pressure on the free streamline must be constant with the same value as the neighboring fluid at rest [5]. Thus since the pressure is constant on the streamline, Bernoulli tells us that the fluid speed is also constant on the streamline. Lastly, a useful identity is that the change in ψ between two streamlines ψ_1 and ψ_2 gives the flux between them,

$$\text{Flux} = \int_C \mathbf{u} \cdot \hat{n} = \int_C (\frac{\partial \psi}{\partial y}, -\frac{\partial \psi}{\partial x}) \cdot (dy, -dx) = \psi_2 - \psi_1. \tag{27}$$

With these additional properties of potential flow noted, let us continue to analyzing the Hodograph method which allows us to solve for the unknown locations of free streamlines using conformal mapping techniques.

We consider a well known example application of the Hodograph method to potential flow out of a slot. An infinite fluid occupies the full upper half plane with a wall at $y = 0$. Centered at the origin is a gap in the wall of length $2a$ (so that the opening is at $x \in (-a, a)$) from where the fluid flows out of as a jet into $y < 0$. The jet thickness far downstream we take to have width $2aQ$ for a contraction ratio Q that we wish to find. From here we follow derivation of the solution given in Chapman's notes [7]. We start by forming the complex potential $w(z) = \phi(x, y) + i\psi(x, y)$ for the associated flow.

The free surfaces of the flow are given by the lines BC and DC'. From Bernoulli we know that the pressure along these surfaces must be constantly equal to the pressure of the surrounding stagnant fluid, which we denote as p_{atm}. Since the velocity must also be constant on the free streamlines we take it as U_∞. For simplicity, the problem is nondimensionalized by scaling z by a and the potential w with $U_\infty a$. As the net flux downstream is now $2Q$, recalling that the difference across streamlines is equal to the flux of the fluid, we take $\psi = -Q$ on ABC and $\psi = Q$ on $A'DC'$. By symmetry this puts the y axis as a streamline with $\psi = 0$. Using a conservation of mass argument, since the flux between the positive x axis and the y axis towards the slot is always Q, and vice-versa for the negative real axis, we have that at infinity in the upper half plane, $\psi \sim Q - 2Q\theta/\pi$. Here $\theta = \arg(z)$. The flow into the origin from the upper half plane corresponds to the potential due to a point sink of strength $4Q$ at the origin, giving

$$w(z) \sim -\frac{2Q}{\pi} \log z + Q \tag{28}$$

as $z \to \infty$ with $\operatorname{Im} z > 0$. Downstream within the jet we want the flow to tend to having constant downward speed, giving $\phi \sim -U_\infty y$ at CC'. In the potential plane, with axes ϕ and ψ,

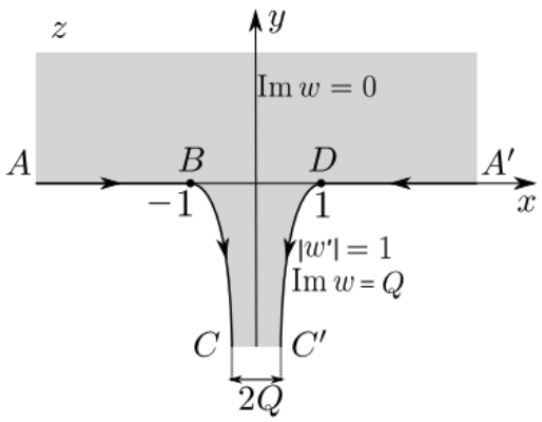

Figure 3: Nondimensionalized model of flow out of a slot. Taken from [7].

the two free streamlines from the z plane become horizontal lines at $\psi = \pm Qi$. Additionally, we can also consider viewing the flow on the hodograph plane, which plots $u = \phi_x$ against $-v = \phi_y$. As the flow in the upper half plane is essentially due to a point sink at the origin the velocity tends to zero at infinity, which puts the line AA' to the origin in the hodograph plane. The free surfaces BC and DC' are mapped to the arcs of the unit circle as the fluid velocity on each starts purely horizontal at points B and D, and turns downwards until it is fully vertical at C and C', respectively. The flow on either of the walls is purely horizontal, thus they are mapped to the x axis. With the hodograph and potential planes, we now consider conformal mappings,

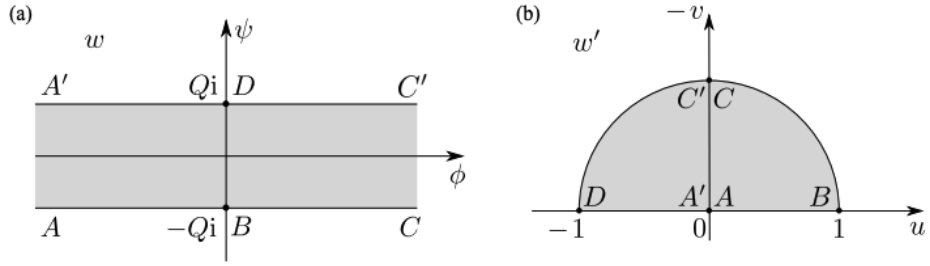

Figure 4: (a) The potential plane $w = \phi + i\psi$ for flow out of the slot. (b) The corresponding hodograph plane $w' = u - iv$. Taken from [7].

$\zeta(w)$ and $\zeta_1(w')$, mapping w and w' to the upper half plane ζ. Critically, we want to find two such mappings that map three points on the boundaries of the hodograph and potential planes to the same points on the boundary of the upper half plane. As noted above, once the location of three points on the boundary have been fixed, the conformal map to the upper half plane is unique and we will end up for an ODE for w given by $\zeta(w) = \zeta_1(w')$ [2].

For the hodograph plane w' to the ζ plane we consider the conformal mapping

$$\zeta(w') = -\left(\frac{1-w'}{w+w'}\right)^2, \tag{29}$$

as shown in Fig. 5. Notably for this map the points in the boundary in the hodograph plane, $A'A, B, CC'$ appear in order on the real axis in the ζ plane at $\zeta = -1, 0, 1$, respectively. Therefore we're looking for a conformal map that takes the locations of $A'A, B, CC'$ in the potential plane w to $\zeta = -1, 0, 1$ in the ζ plane to equate the two mappings. To start, the mapping

$$\zeta_1(w) = ie^{\pi w/2Q} \tag{30}$$

conformally maps the potential plane to the upper half plane. The problem here is that the points along the x axis are not in the same order the mapping ζ. Here we can take advantage of a class of conformal mappings known as bilinear (or Möbius) transformations, which are of the form

$$f(z) = \frac{az+b}{cz+d}, \tag{31}$$

for constant complex numbers a, b, c, d where $ad - bc \neq 0$ [2]. If $c \neq 0$, the transformation is conformal everywhere except $z = -d/c$, which can be seen with a quick inspection of $f'(z)$. Bilinear transformations have many useful properties in conformal mapping methods, but we are most interested in that that for bilinear maps from the upper half plane to the upper half plane, points on the boundary in the domain lie on the boundary after mapping [2]. Now we are looking for a bilinear map $f(\zeta_1)$, such that

$$f(\zeta_1) = \frac{a\zeta_1 + b}{c\zeta_1 + d}, \tag{32}$$

$$f(1) = 0, f(0) = -1, f(\infty) = 1. \tag{33}$$

That map that satisfies this conditions is given by

$$f(\zeta_1) = \frac{\zeta_1 - 1}{\zeta_1 + 1} = f(ie^{\pi w/2Q}). \tag{34}$$

Again, from the Riemann Mapping Theorem since $f(\zeta_1)$ and $\zeta(w')$ both map points $A'A, B, CC'$ in the hodograph and potential planes to the same points on the ζ plane we know that they are identical, providing the ODE

$$\left(\frac{1-w'}{1+w'}\right)^2 = \frac{1 - ie^{\pi w/2Q}}{ie^{\pi w/2Q} + 1} \tag{35}$$

from equations (29) and (34) [2].

We can simplify this ODE as we are only interested in solving it on the free streamlines where we have $|w'| = 1$, as seen on the hodograph plane. Therefore on the free streamlines, w' is of

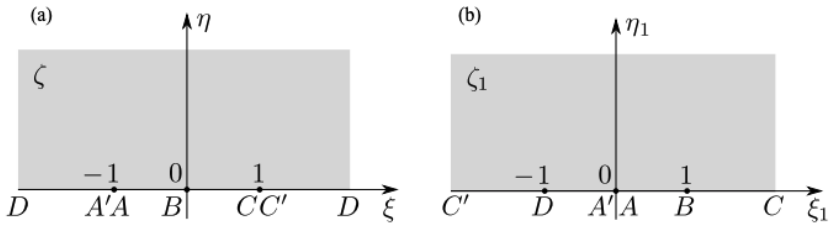

Figure 5: (a) The hodograph plane is mapped to this upper half plane by (29). (b) The potential plane is mapped to this upper half plane by (30). Taken from [7].

the form

$$w' = e^{-i\theta}. \tag{36}$$

Since the hodograph plane plots $(u, -v)$, $-\theta$ is the polar angle in the hodograph plane, meaning that on the free streamline BC we have $-\pi/2 < \theta < 0$. Plugging this expression for w' into (35) gives

$$\frac{1 - ie^{\pi w/2Q}}{ie^{\pi w/2Q} + 1} = \left(\frac{1 - e^{-i\theta}}{1 + e^{-i\theta}}\right)^2 = -\tan^2(\theta/2). \tag{37}$$

This bilinear transformation can be inverted to find

$$ie^{\pi w/2Q} = \sec\theta. \tag{38}$$

See the appendix for the full derivation of equations (37) and (38). The last equation can be differentiated with respect to θ as w is a function of $z = re^{i\theta}$,

$$\frac{i\pi}{2Q} e^{\pi w/2Q} \frac{\mathrm{d}w}{\mathrm{d}z} \frac{\mathrm{d}z}{\mathrm{d}\theta} = \sec\theta \tan\theta. \tag{39}$$

Recalling that $w' = e^{-i\theta}$ and using equation (38) gives $e^{\pi w/2Q} = -i\sec\theta$, we then have

$$\frac{\mathrm{d}z}{\mathrm{d}\theta} = \frac{2Q}{\pi} e^{i\theta} \tan\theta. \tag{40}$$

Thus we have arrived at a first order ODE for $z = re^{i\theta}$ on the free streamline surface. Integrating this equation provides us with a parametric equation $z(\theta)$ for the position of the free surface. To make this integral easier, we split it up into its real and imaginary parts

$$\frac{\mathrm{d}x}{\mathrm{d}\theta} = \frac{2Q}{\pi} \sin\theta, \tag{41}$$

$$\frac{\mathrm{d}y}{\mathrm{d}\theta} = \frac{2Q}{\pi} \sin\theta \tan\theta. \tag{42}$$

Integrating with respect to θ gives that

$$x(\theta) = -\frac{2Q}{\pi}\cos\theta + C_1, \tag{43}$$

$$y(\theta) = \frac{2Q}{\pi}(\log|\sec\theta + \tan\theta| - \sin\theta) + C_2, \tag{44}$$

for unknown constants C_1 and C_2. Recalling that θ corresponds to the angle in the hodograph plane, we can find the unknown constants with the point B where $x = -1, y = 0$ and $\theta = 0$. This produces $C_1 = 2Q/\pi - 1$ and $C_2 = 0$. Traversing down the BC free streamline towards C where we set $x = -Q$, we have $\theta \to -\pi/2$, giving that $y \to -\infty$ and

$$x \to -1 + \frac{2Q}{\pi} = -Q. \tag{45}$$

At last this gives us the contraction ratio of the jet bounded by the two streamlines at $y = -\infty$:

$$Q = \frac{\pi}{\pi + 2} \approx 0.611. \tag{46}$$

Therefore from the opening of width $2a$, the jet eventually shrinks to a width of $2a(0.611)$.

Applying the hodograph method to other problems for finding the locations of free streamlines follows in a similar way. The success of the method comes from the Riemann Mapping Theorem with finding two equivalent conformal maps from the hodograph and potential planes to the upper half plane that produces an ODE to be solved. Now let us proceed to an even more powerful and general result for conformal mapping and its applications.

4 The Schwarz-Christoffel Transformation

Although the Riemann Mapping Theorem's proof of the existence of a conformal map from the unit disc or half plane to a simply connected domain D which is not all of $\mathbb{C}$ is non-constructive, all hope of finding such mappings is not lost [2]. Indeed in the late 1800s, Hermann Schwarz and Elwin Christoffel independently derived a formula for the conformal map from the upper half plane (or unit disc) to the interior of a simple polygon. The result, known as the Schwarz-Christoffel Transformation, we now state.

Theorem 3 ***(Schwarz-Christoffel)*** *Let Γ be the piecewise linear boundary of a polygon in the w plane with vertices $A_1, A_2, \ldots, A_n$ and corresponding interior angles $\alpha_1\pi, \ldots, \alpha_n\pi$. The transformation defined by*

$$\frac{\mathrm{d}w}{\mathrm{d}z} = \gamma(z - a_1)^{\alpha_1 - 1}(z - a_2)^{\alpha_2 - 1}\cdots(z - a_n)^{\alpha_n - 1} \tag{47}$$

where γ is a complex number and $a_1, \ldots, a_n$ are real numbers maps Γ into the real axis of the

z plane and the interior of the polygon to the upper half of the z plane. The vertices of the polygon are mapped to the points $a_1, \ldots, a_n$ on the real axis. The map is an analytic one-to-one conformal transformation between the upper half z plane and the interior of the polygon [2].

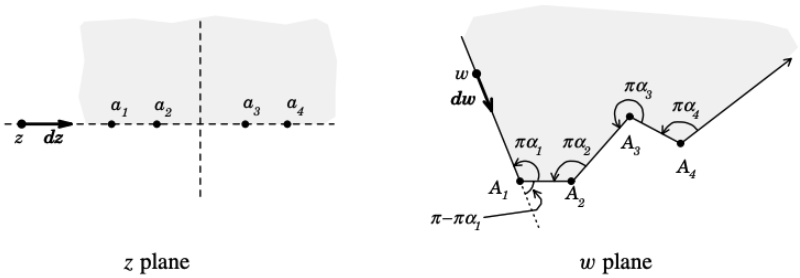

Figure 6: General transformation of the boundary of the real axis in the z plane to the boundary of a polygon in the w plane with selected prevertices $a_1, \ldots, a_n$ on the real axis of the z plane. Taken from [2].

We can also rewrite this in terms of an integral for $w = f(z)$,

$$f(z) = A + C \int_0^z (\zeta - a_1)^{\alpha_1 - 1}(\zeta - a_2)^{\alpha_2 - 1} \cdots (\zeta - a_n)^{\alpha_n - 1} d\zeta \tag{48}$$

for complex constants A and C [8]. Noticeably, the conformal map $f(z)$ from the polygon to the upper half plane is completely defined by the boundary of the polygon, and each a_i is a critical point of the mapping. Vertices at finite locations correspond to $0 < \alpha_i \leq 2$ with $\alpha = 2$ denoting the tip of a slit. For a vertex at infinity, then $-2 \leq \alpha_i \leq 0$. We defer giving a full proof, but instead indulge in a heuristic explanation of the form of (47) as done in Ablowitz and Fokas [2]. The full proof, also given in Ablowitz and Fokas, relies on the Schwarz reflection principle among other theorems in complex analysis that we note in the appendix [2].

Consider a polygon in the w plane with vertices $A_1, A_2, \ldots, A_n$ and corresponding interior angles $\alpha_1\pi, \ldots, \alpha_n\pi$. The objective is to derive an analytic function $w = f(z)$ in the upper half z plane such that $f(z)$ maps the real axis to the boundary of our polygon. As we are interested in the form of (47), we examine the derivative of the mapping $\frac{\mathrm{d}w}{\mathrm{d}z} = f'(z)$, or $dw = f'(z)dz$. While we are traversing the real axis in the z plane to the left of a_i, we have that $\arg(dz) = 0$ where dz is being treated like a vector. On the corresponding boundary of the polygon being traversed we have $\arg(dw) = \text{const}$ until the vertex A_i is reached (assuming A_i is finite). Since the boundary of the polygon is composed of lines connected by vertices, $\arg(dw)$ only changes when a vertex is traversed. Therefore $\arg(f'(z)) = \arg(dw) - \arg(dz) = \arg(dw)$. When the vertex A_i is traversed, $\arg(f'(z))$ changes by the size of the exterior angle of the polygon at A_i, which is given by $\pi(1 - \alpha_i)$. For each vertex, this behavior is given by the function $(z - a_i)^{\alpha_i - 1}$. Traversing the real line to the left of a_i we have $\arg((z-a_i)^{\alpha_i-1}) = (\alpha_i - 1)\arg(z - a_i) = \pi(\alpha_i - 1)$. After a_i has been passed and is to the left of z on the real line this becomes $\arg((z - a_i)^{\alpha_i - 1}) = (\alpha_i - 1)\arg(z - a_i) = (\alpha_i - 1)0 = 0$, as desired. Since $f'(z)$ must express this behavior at every vertex a_i, we are led to conclude that $f'(z)$ is of the form given in (47).

One should be aware that when computing $f(z)$ by integrating (48), multivalued functions often arise due to the exponential terms in the integral [2]. Thus a single branch of the resulting function must be chosen to keep the function analytic in $\mathrm{Im}(z) > 0$. This is achieved by the requirement that $0 < \arg(z - a_i) < \pi$ for all points a_i on the real axis, resulting in $f(z)$ analytic in the upper half plane and each a_i as a branch point of $f(z)$ [2].

Now we will examine a few examples of Schwarz-Christoffel transformations along with an application to fluid flow. We first analyze the Schwarz-Christoffel transformation from the upper half plane to a rectangle, as done in Ablowitz and Fokas (p. 358-359) [2].

Consider a rectangle of width 2 and height s centered along the imaginary axis and on top of the real axis in the w plane. Take k to be any constant real number such that $0 < k < 1$. Since we are mapping from the real axis in the z plane to the interior of the rectangle, we will need to select four points on the real axis to map to each vertex of the rectangle. We will take advantage of the symmetry of the positioning of the rectangle in the w plane, which lets us assume that $f(z)$ is symmetric, $f(-a) = -f(a)$ and $f(0) = 0$ for a real number a. For the vertices, we have $\alpha_1 = \alpha_2 = \alpha_3 = \alpha_4 = 1/2$. On the real axis we select the points $a_1 = -1/k, a_2 = -1, a_3 = 1, a_4 = 1/k$. The natural mapping to the vertices of the rectangle is then a_1 to $A_1(-1+is)$ and a_2 to $A_2(-1)$ with the other two vertex pairs following by symmetry. Since we took $f(0) = 0$, the constant of integration arising in (48) is then zero. With the Schwarz-Christoffel formula we have put together the mapping

$$f'(z) = \frac{\mathrm{d}w}{\mathrm{d}z} = \gamma(z-1)^{-1/2}(z+1)^{-1/2}(z-1/k)^{-1/2}(z+1/k)^{-1/2}. \tag{49}$$

Integrating to find an expression for $f(z)$ gives

$$f(z) = \int_0^z \frac{\gamma}{\sqrt{(\zeta^2-1)(\zeta^2-1/k^2)}} d\zeta. \tag{50}$$

Factoring out a -1 from each product in the denominator along with $1/k^2$ from the second term, and writing $\tilde{\gamma} = k\gamma$ gives

$$f(z) = \tilde{\gamma} \int_0^z \frac{d\zeta}{\sqrt{(1-\zeta^2)(1-\zeta^2 k^2)}}. \tag{51}$$

Fixing that $\sqrt{1} = 1$ provides the correct branch, and that w is real for real z along the real axis past $|z| = 1/k$. Notably, the resulting integral is known as the elliptic integral of the first kind, denoted by $F(z, k)$ [2]. The height of the rectangle, s can be selected by the correct choice of k. A further explanation of that relationship can be found in Ablowitz and Fokas (p. 359) [2]. In the general case for a polygon with $n = 4$ vertices, the prevertices are not ours to choose [8]. Indeed, as noted previously, once three sets of points have been selected to correspond in the z and w planes, the mapping becomes unique thus the remaining vertices are set for which there is no simple analytic method to determine [8].

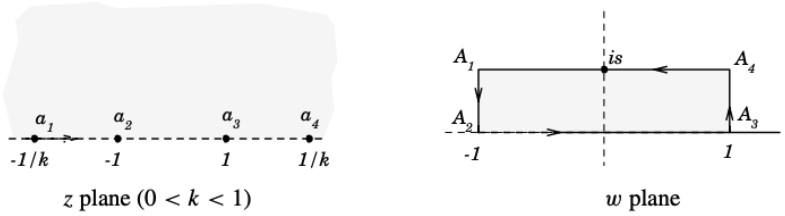

Figure 7: Setup of the Schwarz-Christoffel transformation from the upper half z plane to the interior of the rectangle. The prevertices a_i in the z plane are mapped to the corresponding vertices of the rectangle A_i in the w plane. Taken from [2].

Let us now consider the conformal map from the upper half plane to the exterior of a step as done in Driscoll and Trefethen (p. 17) [8]. This step can be viewed as an unbounded triangle with one vertex at infinity. We pick the two prevertices mapping to the top and bottom of the step to be $z = -1, 1$ respectively. At the top of the step, the opening angle is $3\pi/2$, and the bottom of the step turns by $-\pi/2$. This gives $\alpha_1 = 3/2, \alpha_2 = 1/2$, and since the alphas must sum to 1, we have that α_3 corresponding to the vertex of the triangle at infinity is -1, though this term is already omitted from the integral [8]. Therefore we arrive at the transformation

$$f(z) = A + C \int_0^z \left(\frac{\zeta + 1}{\zeta - 1} \right)^{1/2} d\zeta, \tag{52}$$

$$f(z) = A + C \int_0^z \frac{\zeta + 1}{(\zeta^2 - 1)^{1/2}} d\zeta, \tag{53}$$

$$f(z) = A + C \left[(z^2 - 1)^{1/2} + \cosh^{-1}(z) \right]. \tag{54}$$

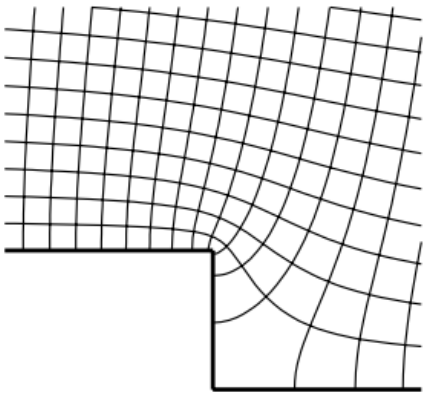

Figure 8: Conformal map from the upper half plane to the exterior of the stem. Vertical and horizontal lines from the upper half plane are mapped to the shown lines. Taken from [8].

As a last example, we solve a potential flow problem via a conformal map provided by a Schwarz-Christoffel transformation, following Ablowitz and Fokas (p. 355-356) [2]. Place a vertical slit in

the w plane arising from $w = 0$ to $w = is$. As the origin in the w plane is traversed twice when moving along the boundary of the slit, we can choose the two prevertices on the real z axis at $z = -1$ and $z = 1$ to correspond to the $w = 0-$ and $w = 0+$ vertices of the slit, respectively. Both of these vertices on the slit correspond to $\alpha = 1/2$. Lastly we select the tip of the slit to correspond to the prevertex $z = 0$ with $\alpha = 2$ since it's an opening of 2π. This translates to the mapping

$$f(z) = A + C \int_0^z \frac{\zeta}{(\zeta+1)^{1/2}(\zeta-1)^{1/2}} d\zeta, \tag{55}$$

$$f(z) = A + C \int_0^z \frac{\zeta}{\sqrt{1-\zeta^2}} d\zeta. \tag{56}$$

Here we are greeted with a familiar integral and can find $f(z)$ explicitly

$$f(z) = A + C'\sqrt{z^2 - 1}. \tag{57}$$

Using our selected prevertex-vertex mappings we know $f(0) = si$ and $f(1) = 0$ so we can solve for A and C',

$$w = f(z) = s\sqrt{z^2 - 1}. \tag{58}$$

We are interested in finding the flow past the slit, given a uniform background flow potential $\Omega(z) = U_0 z$ where U_0 is a constant velocity. Recalling that $\Omega(z) = U_0(\phi + i\psi) = U_0(x + iy)$, we have $\psi = y$ is constant on the real axis when $y = 0$. Additionally, each $y = c$ is a streamline where c is a positive constant. Therefore the real axis is a streamline, ensuring that $\Omega(z)$ is a valid potential flow on the upper real plane. Thus all we need to do now is invert the mapping $w = f(z)$ to map the slit in the w plane to the upper half plane for which we have a valid potential flow for. A simple inversion of (59) provides the correct potential in the w plane given by

$$\Omega(w) = U_0 \left(\left(\frac{w}{s} \right)^2 + 1 \right)^{1/2}. \tag{59}$$

Taking the conjugate of the derivative of $\Omega(w)$ retrieves the velocity field of the fluid in the w plane as desired, which we note becomes infinite at the top point of the slit.

5 Numerical Conformal Mapping

In practice, conformal maps for simple polygons and simply connected domains bounded by a Jordan curve P are found by referring to a catalog or numerically solving for them. In this section we will discuss the standard approaches for numerically computing the Schwarz-Christoffel transformation for a simple polygon and the more general method for the conformal

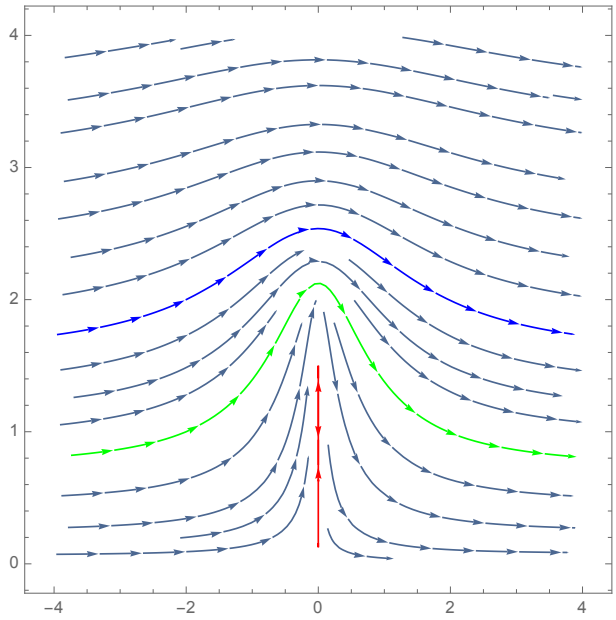

Figure 9: Uniform potential flow past a vertical slit (red) of length 2 and centered on the imaginary axis.

map from an arbitrary simply connected domain.

5.1 Numerical Schwarz-Christoffel

Consider a polygon P with N vertices in the w plane. From the previous section we know that the Schwarz-Christoffel transformation from the upper half plane to P is given by

$$f(z) = w_c + C \int_0^z \prod_{k=1}^{N} (z' - z_k)^{\alpha_k - 1} dz' \tag{60}$$

for complex constants C, w_c and interior angles $\pi\alpha_k$ [9]. The complex variables $z_1, ..., z_N$,C, and w_c are known as the accessory parameters that are to be solved for (giving $2N+2$ unknowns)[9]. Specifically the z_n's on the real axis must be selected such that the map produces the correct side lengths of P and is one-to-one [9]. Here we confront the problem that determining the accessory parameters is intractable analytically, and resort to numerics [9]. Additionally, the problem as it stands has infinitely many solutions [9].

To uniquely determine the map we may fix exactly three points z_k on the real axis, fix one point z_k and select w_c, or fix w_c and $\arg(f'(0))$ [9]. Let us approach the problem in a similar way as Trefethen does, selecting $z_N = 1$, and choosing w_c to be an arbitrary point in P [9]. The aim is to reduce the system to $N-1$ operative equations that can be solved numerically by means of iterative Newton's method. To remove any translational degrees of freedom in the resulting map we require that every connected component of P contain at least one vertex (so even infinitely

straight boundaries must contain a node). Similarly, lets require that at least one component of P contain two finite vertices w_1, w_N, thus eliminating rotational freedom. Since we fixed z_N we can solve for C,

$$C = (w_N - w_c) \Bigg/ \int_0^{z_N} \prod_{k=1}^{N} (z' - z_k)^{\alpha_k - 1} dz'. \tag{61}$$

Next, we can produce two equations (real and complex components) to be satisfied for z_1,

$$w_1 - w_c = C \int_0^{z_1} \prod_{k=1}^{N} (z' - z_k)^{\alpha_k - 1} dz'. \tag{62}$$

Consider the connected components of P, $\Gamma_1, \ldots, \Gamma_m$ in the counterclockwise order. If the last vertex of Γ_l is z_{k_l}, the fact that z_{k_l} must lie on the real axis gives us a complex condition,

$$w_{k_l} - w_c = C \int_0^{z_{k_1}} \prod_{k=1}^{N} (z' - z_k)^{\alpha_k - 1} dz', \tag{63}$$

for $l \geq 2$, providing $2m - 2$ equations. Lastly, the remaining needed $N - 2m - 1$ equations are posed by considering the side lengths of the polygon. For each pair (z_k, z_{k+1}) we require

$$|w_{k+1} - w_k| = \left| C \int_{z_k}^{z_{k+1}} \prod_{k=1}^{N} (z' - z_k)^{\alpha_k - 1} dz' \right|. \tag{64}$$

If the polygon is bounded then the last two side length conditions are not required to reach $N-1$ conditions. Notably, since the integrand in the above integrals is analytic, it can be evaluated over any contour desired [2]. For the far majority of cases, equations (62-63) determine the system with a unique solution that can be solved for [9]. See Trefethen [9] for details on the bad cases. The system we arrived at is non-linear, and may be solved via iterative Newton's method, among other options. After the map is computed, it is relatively easy to analytically transform it to a different domain (i.e. from the upper half plane to the unit circle) by a Möbious transformation [2].

In applications, the inverse map, $z = z(w)$ from the polygon P to the upper half plane is desired. Here we have two distinct options. The mapping $w(z) = w$ for a fixed w can be viewed as a nonlinear equation to be solved for z with iterative Newton's [9]. Alternatively, we can invert the Schwarz-Christoffel formula (49) to arrive at

$$\frac{\mathrm{d}z}{\mathrm{d}w} = \frac{1}{C} \prod_{k=1}^{N} (z - z_k)^{1 - \alpha_k} \tag{65}$$

which can be approached as an ODE for z [9]. If any pair of values (z_k, w_k) is known then we have an IVP that can solved via a selected numerical ODE solver. To find $z = z(w)$ the integral

is numerically computed over any curve from w_k to w which lies in the polygon [9].

5.2 Non-Polygon Domains

To approach the conformal mapping problem for a general simply connected domain bounded by a Jordan curve P, we consider a procedure based on solving Laplace's equation as presented by Trefethen in [10]. Let P bound the domain Ω, an D be the open unit disk. Again we desire a conformal map $f : \Omega \to D$. We assume that $0 \in \Omega$ and restrict f such that $f(0) = 0$ and $f'(0) > 0$. We start with the ansatz that f is of the form

$$f(z) = ze^{u(z)+iv(z)} \tag{66}$$

where $u(z)$ and $v(z)$ are real harmonic conjugates in Ω. By the Osgood-Carathéodory theorem we have that f can be extended to map the boundaries of the domain given by P to the boundary of the unit disc ($z = e^{i\theta}$) in a conformal and one-to-one way [2]. Now, consider $g(z) = \log(f(z)/z)$, which is nonzero, analytic on Ω, and continuous on $\overline{\Omega}$. On P, $g(z)$ has the real part $-\log|z|$ and imaginary part 0 at $z = 0$. Therefore since u and v are harmonic conjugates, we have that u is the unique solution of Laplace's equation,

$$\Delta u(z) = 0; \tag{67}$$

$$u(z) = -\log|z|, z \in P. \tag{68}$$

Thus we have arrived at finding the Green's function $u(z) + \log|z|$ on Ω with respect to the point $z = 0$. After finding $u(z)$ it's harmonic conjugate $v(z)$ can be easily computed to retrieve $f(z)$.

For simply connected domains with smooth boundaries, the solution $u(z)$ to the Laplace problem can be approximated well by polynomials [11]. We follow suit and let u be approximated as

$$u(z) \approx \mathrm{Re} \sum_{k=0}^{n} c_k z^k, \tag{69}$$

for a selected degree n and complex coefficients c_k [11]. Expanding each of the complex coefficients gives

$$u(z) \approx \mathrm{Re} \sum_{k=0}^{n} (a_k \,\mathrm{Re}(z^k) - b_k \,\mathrm{Im}(z^k)) \tag{70}$$

with $b_0 = 0$. This summation provides $N = 2n + 1$ unknowns that are to be determined by sampling the function $-\log|z|$ at $M >> N$ points on P and solving the resulting $M \times N$ matrix least squares problem [11]. Once the coefficients c_k's are found we have $u(z)$ and can

approximate its harmonic conjugate $v(z)$ with the series

$$v(z) \approx \operatorname{Re} \sum_{k=0}^{n} (a_k \operatorname{Im}(z^k) - b_k \operatorname{Re}(z^k)). \tag{71}$$

Finally, equation (6) gives us $f(z)$ as desired. The resulting degree of the polynomial $u(z)$ usually has to be high to achieve desired accuracy [10]. Further, the monomials $1, z, z^2, \ldots$ are a very ill-conditioned basis, thus it is best to instead use orthogonal polynomials over P, which can be done via the Arnoldi iteration while solving the least squares problem [12]. Additionally, as n normally has to be high (in the hundreds to thousands) for smooth domains, a simplified representation of the resulting $f(z)$ is desired for improved performance [10]. As put forth by Trefethen, the AAA algorithm can be utilized to compress f to a much more compact form as a rational function [11, 13]. The AAA algorithm produces an equivalent approximation of f with Barycentric form,

$$f(z) = \frac{\sum_{j=0}^{n} \frac{w_j}{z - z_j} f(z_j)}{\sum_{j=0}^{n} \frac{w_j}{z - z_j}}, \tag{72}$$

$$w_j = \frac{1}{\prod_{k \neq j} (z_j - z_k)}, \tag{73}$$

which is similar in nature to a Lagrange interpolating polynomial, but with significantly improved computational cost of evaluating $f(z)$ ($O(n^2)$ to $O(n)$) [13]. Overall, this algorithm works well for domains Ω bounded by smooth curves P [10]. Once Ω begins to contain sharp corners, the degree n required to accurately resolve the corner with f grows quickly to unreasonable values [10]. The above algorithm is available in the numerical computation package Chebfun, for which we give an example of below in Fig. 10 [14]. The default algorithm for numerically computing conformal maps with Chebfun's 'conformal' command instead discretizes the Kerzman-Stein integral equation, not discussed here [10]. Lastly, Trefethen showed that the above algorithm can be improved upon for arbitrary domains with sharp corners that introduce singularities on the boundary (including polygons) by instead seeking a representation of $u(z)$

$$u(z) \approx \operatorname{Re} \left[\sum_{j=1}^{n_1} \frac{a_j}{z - z_j} + \sum_{j=0}^{n_2} b_j z^j \right], \tag{74}$$

for complex coefficients a_j and b_j [10]. The first sum in brackets are of the form of rational functions, which can approximate certain singularities with root exponential convergence $O(C^{-\sqrt{n}})$ in the supremum norm of the error, given that the poles z_j are exponentially clustered near the corners [15]. The polynomial portion of the sum will be still be implemented via the Arnoldi factorization [10]. An example of this algorithm for a domain with corners is given in Fig. 11.

Let us summarize the above. The problem of numerically computing a conformal map from a simply connected domain bounded by a Jordan curve can be formulated in terms of solving Laplace's problem [10]. For domains bounded by smooth curves without 'corners', representing

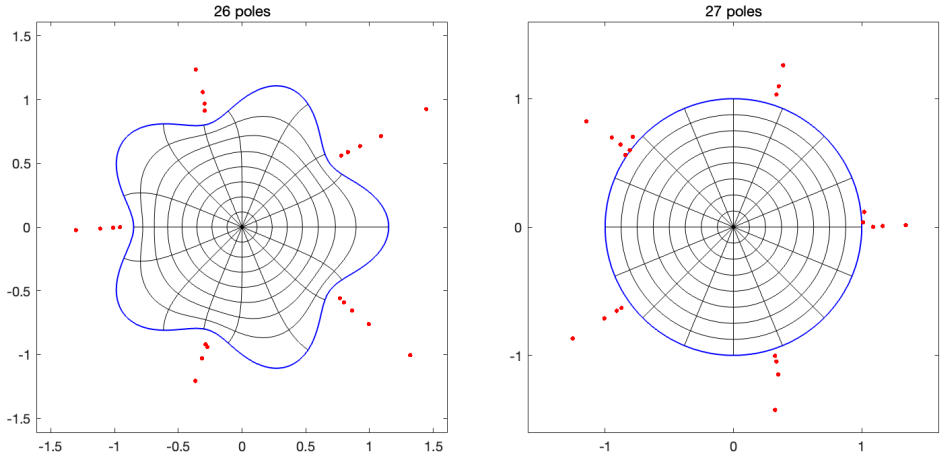

Figure 10: Conformal map of a smooth domain to the unit disk, computed to around 5-digit accuracy via the Chebfun 'conformal' command with the polynomial representation option [14]. As the dimples in the domain move towards the origin the polynomial representation of $u(z)$ requires a very high degree polynomial and subsequently fails. The red dots mark poles of the representations of f and f^{-1}.

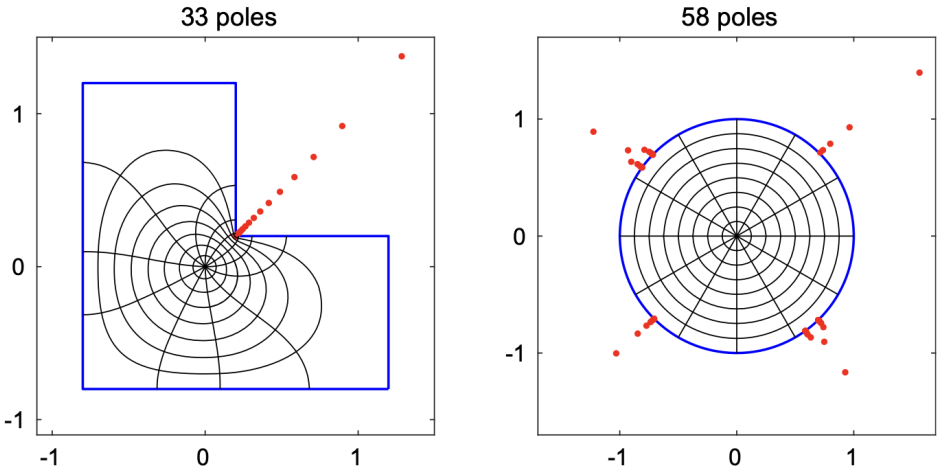

Figure 11: Conformal mapping of an L-shaped domain by approximating $u(z)$ with the form given in (74). The map f is non-singular at the normal corners and poles cluster only at the reentrant corner. The strictly polynomial representation of f would fail for this domain due to the existence of corners. Taken from [10].

the solution to Laplace's problem as a polynomial performs as desired [11]. Domain boundaries exhibiting significant deformations to sharp corners are served much better by representing the solution as a rational function added to a polynomial [10, 15]. In both cases the resulting conformal map $f(z)$ can be efficiently represented by rational functions via the AAA algorithm [13].

References

[1] D. J. Acheson, *Elementary Fluid Dynamics.* Oxford University Press Inc., New York, 1990.

[2] M. J. Ablowitz and A. S. Fokas, *Complex Variables: Introduction and Applications.* Cambridge University Press, 2003.

[3] Z. Nehari, *Conformal Mapping.* McGraw-Hill, 1952.

[4] C. Carathéodory, "Zur ränderzuordnung bei konformer abbildung," *Göttingen Nachrichten*, pp. 509–518, 1913.

[5] L. Milne-Thompson, *Theoretical Hydrodynamics.* Dover Publications, Inc., 1968.

[6] I. Currie, *Fundamental Mechanics of Fluids, Third Editition.* Taylor Francis, 2003.

[7] J. Chapman, "C5.6 applied complex variables, course notes," pp. 46–50, 2022.

[8] T. Driscoll and L. Trefethen, *Schwarz-Christoffel Mapping.* Cambridge University Press, 2002.

[9] L. N. Trefethen, "Numerical computation of the schwarz-christoffel transformation," *SIAM J. Sci. Stat. Comput.*, vol. 1, p. 82–102, 1980.

[10] L. Trefethen, "Numerical conformal mapping with rational functions," *Comput. Methods Funct. Theory*, vol. 20, p. 369–387, 2020.

[11] L. N. Trefethen, "Series solution of laplace problems," *ANZIAM J.*, vol. 60, p. 1–26, 2018.

[12] L. Trefethen and D. I. Bau, *Numerical Linear Algebra.* SIAM, 1997.

[13] Y. Nakatsukasa *et al.*, "The aaa algorithm for rational approximation," *SIAM J. Sci. Comput.*, vol. 40, pp. A1494–A1522, 2018.

[14] T. Driscoll *et al.*, "Chebfun user's guide," 2014.

[15] A. Gopal and L. Trefethen, "Solving laplace problems with corner singularities via rational functions," *SIAM J. Numer. Anal.*, vol. 57, pp. 2074–2094, 2019.

6 Acknowledgements

The author would like to thank his two roommates Dmitry Zverevich and Owen Eskandari for their proofreading and content suggestions along with Thomas Chandler for recommending useful background literature for this work.

7 Appendix

7.1 Flow through a slit

We start with

$$\frac{1-ie^{\pi w/2Q}}{ie^{\pi w/2Q}+1}=\left(\frac{1-e^{-i\theta}}{1+e^{-i\theta}}\right)^2. \tag{75}$$

Inside the parenthesis we can multiply the numerator and denominator of the expression by $e^{i\theta/2}$ to get

$$\frac{1-ie^{\pi w/2Q}}{ie^{\pi w/2Q}+1}=\left(\frac{e^{i\theta/2}-e^{-i\theta/2}}{e^{i\theta/2}+e^{-i\theta/2}}\right)^2. \tag{76}$$

Recalling that $e^{i\theta/2}-e^{-i\theta/2}=2i\sin(\theta/2)$ and $e^{i\theta/2}+e^{-i\theta/2}=2\cos(\theta/2)$ produces

$$\frac{1-ie^{\pi w/2Q}}{ie^{\pi w/2Q}+1}=\left(\frac{i\sin(\theta/2)}{\cos(\theta/2)}\right)^2=-\tan^2(\theta/2) \tag{77}$$

as desired. Now consider the first and third expressions, we can add one to each side,

$$\frac{2}{ie^{\pi w/2Q}+1}=-\tan^2(\theta/2)+1. \tag{78}$$

Taking the inverse gives

$$ie^{\pi w/2Q}=\frac{2}{1-\tan^2(\theta/2)}-1, \tag{79}$$

$$ie^{\pi w/2Q}=\frac{\tan^2(\theta/2)-1}{1-\tan^2(\theta/2)}. \tag{80}$$

We recall the identity

$$\tan^2(\theta/2)=\frac{1-\cos(\theta)}{1+\cos(\theta)}. \tag{81}$$

With this we can expand (52) to

$$ie^{\pi w/2Q} = \frac{1 - \frac{1-\cos(\theta)}{1+\cos(\theta)}}{1 + \frac{1-\cos(\theta)}{1+\cos(\theta)}}, \tag{82}$$

$$ie^{\pi w/2Q} = \frac{\frac{2}{1+\cos\theta}}{\frac{2\cos\theta}{1+\cos\theta}}, \tag{83}$$

$$ie^{\pi w/2Q} = \frac{1}{\cos\theta} = \sec\theta, \tag{84}$$

as desired.

7.2 Schwarz-Christoffel Extras

(Schwarz Reflection Principle) Suppose that the domain D has part of the real axis as part of its boundary. Assume $f(z)$ is analytic in D and is continuous as z approaches the line segments $L_1, \ldots, L_n$ of the real axis and that $f(z)$ is real on these segments. Then $f(z)$ can be analytically continued across $L_1, \ldots, L_n$ into $\tilde{D}$ [2].

With linear transformations and rotations in the z and w plane, this result can be extended to line segments not on the real axis [2].

(Osgood-Carathéodory Theorem) If D is bounded by a simple closed contour, then it is possible to extend the function f mapping D conformally onto the open unit disk in such a way that f is continuous and one to one on the boundaries [2].